THE IMPACT OF CHLORIDE INDUCED CORROSION AND LOW CYCLE FATIGUE ON REINFORCING STEEL

ВОЗДЕЙСТВИЕ ХЛОРИДНО ВЪЗВАННОЙ КОРРОЗИИ И НИСКОЦИКЛОВОЙ УСТАЛОСТИ У АРМИРОВОЧНОЙ СТАЛИ

Ch. Alk. Apostolopoulos[1], D. Michalopoulos*
DEPARTMENT OF MECHANICAL ENGINEERING AND AERONAUTICS, UNIVERSITY OF PATRAS, PATRAS, GREECE 26500.
*Corresponding author. Tel./Fax 0030-2610-996204 ,
E-MAIL : [1] CAPOSTOLO@TEE.GR , * MIXALOP@MECH.UPATRAS.GR

***Abstract**: Reinforced concrete is affected by chloride corrosion and the original mass of the steel reinforcement is reduced thus endangering the integrity and lifetime of the structure. An experimental study was conducted on BSt500$_s$ steel which showed that the level of corrosion had a direct impact on the mass loss and low cycle fatigue (LCF). Strain controlled LCF testing under ±1 and ±2.5% constant amplitude strain showed that the corroded bars exhibit gradual reduction in available energy, remaining life and their load bearing ability. Pits and notches were formed on the corroded steel surface and stress concentration points were developed which are highly localized at imperfections and especially at the rib bases. The experimental investigation of the specimens subjected to LCF showed that the life expectancy, the remaining energy density and the strength properties were reduced as a result of the formation of pits and notches combined with the mass loss and reduction of the exterior hard layer of martensite. Seismic design that does not account for reduction of the load bearing ability, life expectancy and cumulative plastic deformation of the steel due to the loading and corrosion history that a structure will suffer under severe weather and ground motion could lead to unpredictable performance.*
KEYWORDS: MASS LOSS; CHLORIDE CORROSION; LOW CYCLE FATIGUE; BSt500$_s$ STEEL ; PLASTIC DEFORMATION.

1. Introduction

Corrosion deterioration of the steel reinforcement in concrete structures is a serious problem with high economic impact. Structures exposed to harsh environments such in coastal sites or containing deicing salts are particularly at risk. Since the steel reinforcement cannot be inspected visually, corrosion often remains undetected until extensive cracking or spalling has occurred. This type of damage can reduce the service life of the structural member and can also create a safety hazard. Reinforcement embedded in concrete will not corrode under ideal conditions since concrete having a pH of approximately 12.5-13 provides a protective environment and formation of a thin film of passivating iron oxide on its surface. The two processes leading to a breakdown of the passivating film and initiation of corrosion, which are essentially of the same type, are:

a) Development of an acidic environment when carbon dioxide from the air mixes with water in the concrete pores (known as carbonation) that removes the passivating layer and

b) The passivating layer can become permeable due to the presence of chloride ions that penetrate into the concrete from seawater, salt and saltwater, deicing chemicals, brackish water or spray from these sources and marine environments [1-5].

Carbonation reduces the pH to approximately 8 or 9, destabilizes the oxide film and with adequate supply of oxygen and moisture initiates corrosion. The penetration of concrete structures by carbonation is a slow process, the rate of which is determined by the penetration of carbon dioxide into the concrete and also its degree of porosity and permeability [3,6]. Chloride ion corrosion is initiated by their entrance into the concrete from de-icing salts or from seawater in coastal sites. The chlorides within the salt act as a catalyst in the natural corrosion process. At the start of corrosion the reinforcement is eventually replaced by rust, a porous product with volume of 3-8 times higher than the reinforcing steel. As corrosion continues the rust exerts tensile forces on the surrounding concrete and causes delamination along the steel-concrete interface. Electrochemical corrosion starts due to the existence of an anode a cathode an electrolyte and a metallic path. The alkaline solution that protects the rebar remains stable in the alkaline concrete environment, but begins to deteriorate when the pH of the pore solution drops below 11 [7-10].

Rust occurs because of differences in electrical potential between small areas on the steel surface involving anodes, cathodes and an electrolyte. This results in crack formation from the steel bar to the concrete surface or between bars allowing oxygen and moisture to attack the bars faster and increase the corrosion rate. The rust reduces the bond strength and results in the loss of steel-concrete composite action, which affects the serviceability and performance of structures [3,10-13].

In coastal locations the climatic conditions constitute one of the most aggressive environments for concrete structures due to the severe ambient salinity, high temperature and humidity and also due to the ingress of chlorine through wind borne salt spray [7-8]. Chloride corrosion leads to concrete cracking, spalling, destruction of the protective steel barrier and formation of pits, notches and cavities on the steel surface [2-3,9].

The current design codes do not account for corrosion of steel since they are unable to quantify it. The reduction in the structural performance of reinforced concrete members due to corroded steel is caused by the loss in the effective cross-sectional area of concrete due to cracking in the cover concrete, loss in the mechanical properties and performance of reinforcing bars due to reduction of their cross-sectional area and also loss of bonding[7,10,14-18]. Seismic loads act on the load bearing elements of structures in the form of high strain reversals, which can be simulated as single axis LCF.The Fourier spectra of ground movement during an earthquake that occurred in Japan showed that the loading was cyclic and the frequency corresponding to the maximum amplitude was approximately 2 Hz. Investigation of the catastrophic earthquake of Tang Shan in China confirmed that the failure mode of the building structural steel was LCF [4].

Earthquakes inflict cumulative damage on reinforced concrete structures but most codes do not explicitly take it into account. In current design practice a displacement ductility factor is used which however fails to account for the accumulated damage since it is implicitly assumed that structural damage occurs only due to the maximum response deformation and is independent of the number of non-peak inelastic cycles or strain energy dissipation. However all inelastic cycles must be considered contributory to damage the accumulation of which may become important depending on the characteristics of the ground motion. During strong earthquakes, yielding structures undergo increased number of cycles into the inelastic range and the accumulated damage may significantly affects their overall performance. This type of damage may also arise from multiple seismic events, in which case, a series of pre or post shocks in combination with the main shock may be treated as a single event of extended duration. Assessment of seismic damage is usually assumed to be similar to metal fatigue under variable amplitude cyclic loading. The level of corrosion combined with the LCF is an issue of great concern for designers since each one of these factors affects the rebar durability and performance and shortens the design life of structures [4-6,19-22].

The results of an experimental investigation are presented in this paper showing the influence of chloride induced corrosion on the mass loss and LCF testing at constant strain amplitude of BSt500**s** tempcore 12 mm diameter steel specimens, which are important for the assessment of the safety and residual life of corroded structures that are located within seismic zones such as Greece, Japan, Western United States, etc.

2. Preconditions and means for solving the problem

2.1. Corrosion induced mass loss

Ribbed steel bars of 12 mm diameter were artificially corroded in a salt spray corrosion chamber, according to ASTM B117-94 standard, for 10, 20, 30, 45, 60 and 90 day. The spray solution was 5% sodium chloride and 95% distilled water, with pH range of 6.5-7.2 and spray chamber temperature of $35\pm^{1.1}_{1.7}$ ^oC for different durations so that different corrosion levels were obtained.

BSt500**s** steel in maximum permissible values of the final product contains C=0.240%, P=0.055%, S=0.055% and N=0.013% and its mechanical properties are shown in Table 1.

Table 1. Mechanical properties of steel BSt500s specimen

Yield stress (MPa)	Tensile strength (MPa)	Elastic modulus (GPa)	% Elongation after breaking
Ribbed bar ≥ 500	≥ 550	200	≥12

The properties of the corroded material were compared against the requirements set in the standards for involving steels in reinforced concrete structures. It should be emphasized that accelerated salt spray corrosion tests on bare bars and steel embedded in concrete theoretically lead to different results, but they represent results represent a good first approximation of the influence of both plastic deformation and quick corrosion on steel ductility properties versus exposure of embedded steel in a natural corrosive environment which would require years to reach similar levels of deterioration since the concrete delays the chloride penetration depending on its physical and chemical characteristics. When the chlorides reach the reinforcement and exceed a critical concentration level then the corrosion process takes place almost similarly with the case of bare bars.

Pitting was observed to have started progressively on the specimens after 10, 20 and 30 days corrosion level which became progressively more severe. After salt spray exposure the specimens were washed with clean water according to ASTM G 1-72 procedure in order to remove any left over salt deposits and then dried. The pitting developed on the steel surfaces even after removal of the rust is shown in Fig. 1.

non corroded **30 days corrosion**

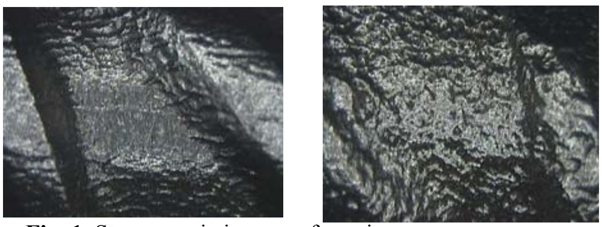

Fig. 1. Stereoscopic images of specimens

The relatively large pits at 30 days of salt spray exposure suggest that these are the active sites at which corrosion is primarily taking place. Pitting appeared to be initiated at the reinforcement veins of the steel bars and proceeded to the intermediate space. The corrosion process created pitting and formed cavities and notches on the steel surface and especially in the rib bases, which became progressively more severe as the corrosion level increased, reaching an average pit depth after 90 days, according to ASTM G46-94 standard guide for examination and evaluation of pitting corrosion, of approximately 0.25 mm with maximum value of 0.50 mm. The degree of corrosion was measured as the percentage mass loss given by the ratio of the difference between the initial and final masses (M_i - M_f), before and after completion of the corrosion process, divided by M_i , multiplied by 100. The remaining mass loss and remaining diameter versus corrosion level for the steel specimens is shown in Table 2. The area A**s** used in the fatigue calculations was determined according to DIN 488-3 specification from:

(1) $$A_s = \frac{1.274 \times M_f}{l}$$

where A**s** is in mm2, M_f is in g and l is the length in mm.

Table 2. Mass loss and remaining diameter at different corrosions

	Exposure to salt spray corrosion environment						
Exposure time[days]	0	10	20	30	45	60	90
Mass loss [%]	0	1.35	2.00	3.03	4.89	6.65	10.40
Diameter [mm]	12.00	11.92	11.88	11.82	11.70	11.59	11.36

2.2. Low Cycle Fatigue

The steel specimens were subjected to uniaxial sinusoidal loads of 1Hz frequency and constant strain amplitude of ±1 and 2.5% after being exposed to salt spray for different durations. A total of 42 low cycle fatigue tests were conducted, 3 for each corrosion level at 0, 10, 20, 30, 45, 60 and 90 days. The length of the 12 mm diameter specimens was 172 mm and the free length between grips was set at an empirical value of 6x12 = 72 mm, since it represents typically the free bar length between stirrups in critical regions of columns in seismic areas. The specimens were subjected to LCF testing without modifications of their cross sectional area since this would alter the nature of the material thus giving misleading results. The analytical expression for total strain is given by [24]:

(2) $$\frac{\Delta\varepsilon_t}{2} = \frac{\Delta\varepsilon_e}{2} + \frac{\Delta\varepsilon_P}{2} = \frac{\sigma'_f}{E}(2N)^b + \varepsilon'_f(2N)^c$$

where $\Delta\varepsilon_t$, $\Delta\varepsilon_e$ and $\Delta\varepsilon_p$ are the total, elastic and plastic strain amplitudes respectively, as shown in the steady state loops of Fig. 2, $\boldsymbol{\varepsilon'_f}$ and $\boldsymbol{c}$ are the fatigue ductility coefficient and exponent respectively. $\boldsymbol{\sigma'_f}$ and **b** are the fatigue strength coefficient and exponent respectively and E is the modulus of elasticity.

Figure 2 shows representative typical hysteresis loops for LCF for different corrosion levels and ±1 and ±2.5% applied strain, where progressive reduction of stress is observed. The total dissipated energy density was evaluated as the sum of the areas formed within the hysterisis loops. This measures the capacity of the material to absorb energy during seismic activity. After evaluating the total energy absorbed the remaining energy density was plotted after each cycle as a function of the number of subjected cycles [8,21-26].

Even though random non corroded and corroded specimens are represented it is clearly shown that plastic deformation ($\Delta\varepsilon_p$) is predominant. Therefore since the plastic deformation ($\Delta\varepsilon_p$) occupies the 33.5% of the applied width at ±1% strain level as expected, this amount is increased to 66.5% when the strain level is ±2.5%. The measured plastic deformation corresponds approximately to the average life expectancy of the material. Cycling with large or small strain amplitudes are additive and highly reduce the useful life expectancy of steel in accordance to plasticity theory. Knowing the mechanical behaviour of the gradually corroded steel and as shown in Fig. 4, the reduction in ductility properties such as elongation and energy density, is evident. It is finally apparent that the reduction of the useful life of steel is closely related to the loading history, the width of the subjected strain and the imposed corrosion level [8,14,21,24,27-30]. Since the LCF tests were performed at constant strain amplitude, the maximum resisting force exerted by the specimens for each cycle was gradually reduced. Furthermore, an overall reduction of the applied force was observed for the pre and post corroded specimens which was expected since the cross sectional area was reduced with advancing corrosion and imposed cycling, contrary to the expectation that the reinforcing steel is expected to carry a constant load throughout its service life.

Typical hysterisis loops of non-corroded and corroded specimens are shown in Fig. 2 where progressive reduction of stress is observed. From the LCF tests, the total dissipated energy density was evaluated as the sum of the areas formed within the hysterisis loops. This is a measure of the capacity of the material to absorb energy during seismic activity. After evaluating the total energy absorbed the remaining energy density was plotted after each cycle as a function of the number of subjected cycles. Corrosion has a direct effect on the exponential coefficients **c** and **b** of the reinforcing steel bars and their average value (for each group of three measurements) was calculated from the LCF test results for each corrosion level and applied strain as shown in Table 3 and Fig. 3.

The variation is especially more evident in coefficient **c** since it determines the material behaviour in the plastic region.

Seismic damage assessment is usually assumed to be similar to metal fatigue under variable amplitude cyclic loading. Seismic damage, however, is normally assessed in terms of only the plastic strain component since a relatively small number of load cycles is imposed by the earthquake ground motion.

Assuming a correspondence between steel bar material and structural damage [21,23] the low-cycle fatigue model under constant displacement amplitude cycles may be written as:

$$\Delta_m - \Delta_y = (\Delta_{um} - \Delta_y)(2N_f)^c \quad (3)$$

Where Δ_m = peak displacement under constant amplitude cycles Δ_y = yield displacement; Δ_{um} = ultimate displacement under monotonic loading; N_f = number of cycles to failure; c = low-cycle fatigue constant (-0.5 to -0.8); Δ indicates displacement with plastic deformation.

Knowing the significance of the plastic strain to the life expectancy of steel reinforcement and from Fig. 2 it can be seen for example that for 1% applied strain the plastic deformation ($\Delta\varepsilon p$) in the non corroded case occupies approximately 22% of the width of the loop while after 90 days corrosion level it increases to approximately 29%. For 2.5% applied strain the corresponding values for plastic deformation ($\Delta\varepsilon_p$) in the non corroded case and 90 days corrosion level are approximately 63 and 67% of the width of the loop. Therefore corrosion and applied strain levels are the predominant factors to material inflicted damage.

Figures 5 and 6 show the correlation of the maximum tensile-compressive force versus applied cycles for ±1 and 2.5% strain level for three random specimens.

Table 3 Effect of corrosion on coefficients **c** and **b**

Strain amplitude		± 1%		± 2.5%	
Coefficients		c	b	c	b
Corrosion level	Samples	-0.5460	-0.0786	-0.5540	-0.0900
	10 days	-0.5670	-0.0786	-0.5670	-0.0890
	20 "	-0.5650	-0.0795	-0.5850	-0.0880
	30 "	-0.5650	-0.0812	-0.5770	-0.0922
	45 "	-0.5800	-0.0833	-0.5830	-0.0960
	60 "	-0.5930	-0.0881	-0.6000	-0.1010
	90 "	-0.6250	-0.0993	-0.6170	-0.1080

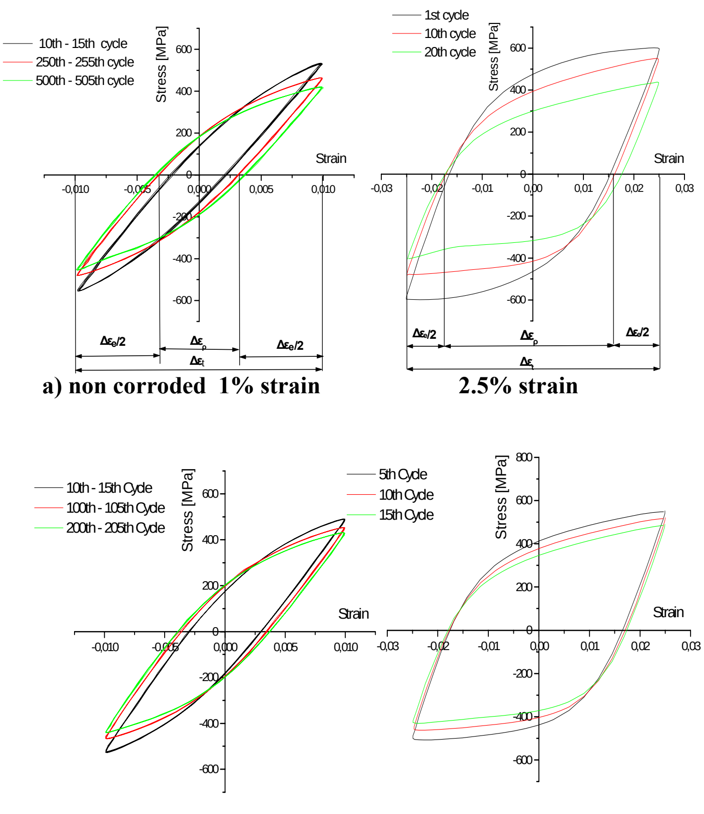

a) non corroded 1% strain **2.5% strain**

b) 90 days 1% strain **2.5% strain**

Fig. 2. Typical LCF stress-strain diagrams, at ±1 and 2.5% applied strain, showing hysterisis loops for initial, middle and final cycles for non corroded and 90 days corroded steel

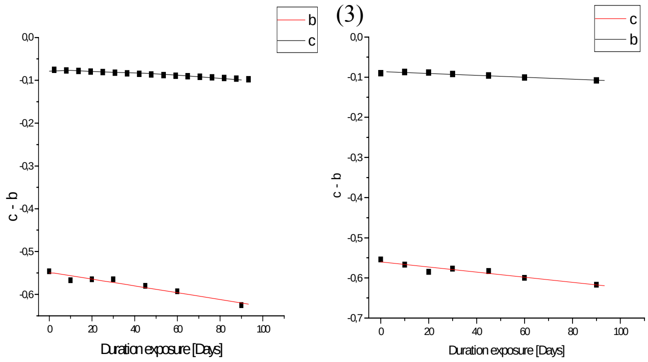

1) 1% strain level **2)** 2.5% strain level

Fig. 3. Variation of coefficients **c** and **b** versus corrosion duration

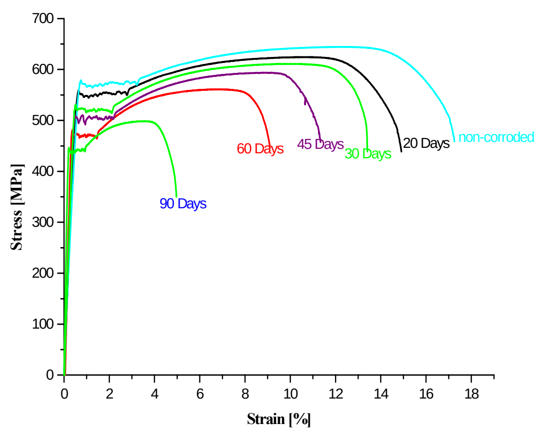

Fig. 4. Reduction of elongation and energy density

of different corrosion levels

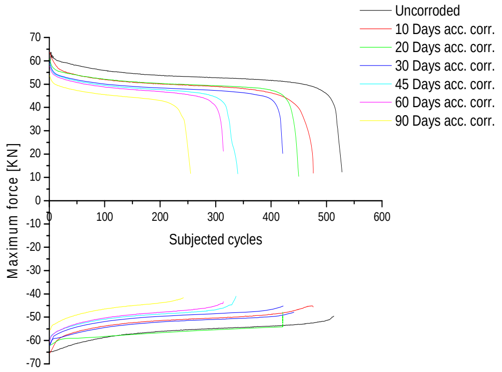

Fig. 5 Correlation of maximum tensile-compressive force versus applied cycles for ±1% strain level

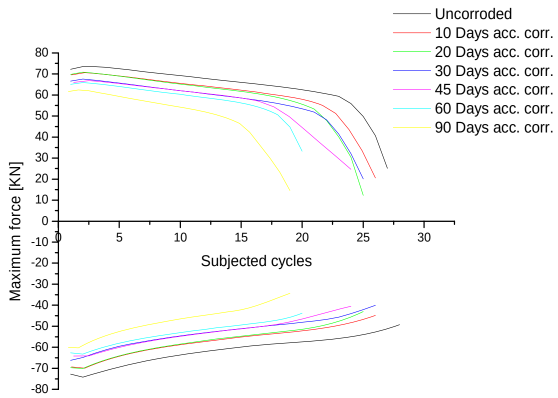

Fig. 6 Correlation of maximum tensile-compressive Force versus applied cycles for ±2.5% strain level

3. Results and discussion

The experimental results represent a good indication of the influence of plastic deformation and corrosion on steel ductility properties. The accelerated chloride corrosion testing of bare steel bars represent a good first approximation of the influence of both plastic deformation and quick corrosion on steel ductility properties versus exposure of embedded steel in a natural corrosive environment which would require years to reach similar levels of deterioration.

Corrosion was found to be detrimental for the integrity of steel while pitting was evident after a few days of salt spray and became progressively more severe as the corrosion level increased, as shown in Fig. 1. As the steel surface became rougher cavities and notches were formed which reduced the steel diameter. Considerable reduction in the fatigue limit took place since the mass loss led to reduction of the exterior hard layer of martensite and drastic drop in the energy density of the corroded specimens thus developing stress concentration points which are highly localized at imperfections and especially in the pits and notches of the rib bases of the corroded steel. Thus the increased corrosion led to a decrease of the useful life of steel. Table 2 shows the mass loss and remaining steel bar diameter versus corrosion level. It was observed that a small mass loss created great reduction in the strength and life expectancy of steel. The rib height was also measured during the different levels of corrosion and at 90 days, corresponding to 10.40% mass loss, the average height of the ribs was reduced by approximately 80%.

The stress-strain behaviour shown in Fig. 2 indicates data for reinforcing steel subjected to reversed cyclic strain with symmetric inelastic strain intervals. In engineering practice such data exhibit particular response characteristics that are not obviously realized by tensile tests. Important characteristics of response of the specimens shown in Fig. 2 and 4 include :

a) Loss of linearity during unloading, known as Bauschinger effect, prior to achieving the yield strength in the opposite direction.

b) Exhibition of isotropic strain hardening characterized by increasing strength under increasing inelastic strain demand. This is observed under cyclic as well as monotonic loading.

c) The initial tangent to the unloading stress-strain response is slightly less than the initial elastic stiffness.

d) Exhibition of cyclic strain softening, known also as reduced tangential stiffness under multiple cycles to particular strain limits.

Figure 3 shows that there is a direct effect on the exponential coefficients **c** and **b** of the reinforcing steel bars and their average value was calculated from the LCF test results for each corrosion level and applied strain.

Figure 4 shows the stress-strain variation versus corrosion level and the energy density as the area under these curves. It can be observed that as the corrosion level increases not only the strength properties, of yield and fracture points, but also the ductility properties such as energy density and elongation to fracture decrease. In severe climates and seismic areas steel bars must have great amounts of energy density, which characterizes the resistance to failure and may be used to evaluate the fracture under both static and dynamic fatigue loading conditions [14,31]. Significant reduction in energy density was observed as the corrosion level increased. The non corroded material has greater energy density than any of the corroded bars, as shown by the area under the stress-strain curve. For smaller strains and longer lives the elastic strain component is more predominant while for larger strains and shorter lives the plastic component is predominant. At larger strains the life expectancy of smooth specimens is extended due to ductility while at smaller strains stronger material is required. From strain versus life expectancy tests of pre and post corroded specimens it was realized that life expectancy is indirectly dependant on the strain amplitude.

The experimental results of uniaxial fatigue tests have shown an overall degradation of the corroded BSt500$_s$ steel reinforcing bars. The formation of an oxide layer on the surface of the specimens made them rougher by forming pits, notches and cavities and thus allowing formation of stress concentration points leading to cumulative damage under alternating fatigue loading. Furthermore, the oxide layer reduced the nominal cross sectional area of the specimens. Considerable degradation of the steel specimens due to corrosion creates a drop in energy density, Fig. 5, combined with the gradual loss of the exterior hard layer of martensite. Corrosion initiation in chloride environments as well as fatigue crack initiation and propagation are phenomena known to be of stochastic nature. Reproducibility of the results was found to be within acceptable levels.

Figures 5 and 6 show the correlation of the maximum tensile-compressive force versus applied cycles for ±1 and 2.5% strain level for three random specimens. It can be seen that as the corrosion level increases the maximum force that the steel bar can sustain, both in tension and compression, decreases. Also as the strain level increases from 1 to 2.5% the maximum force decreases by approximately 8-14 %.

4. Conclusions

Corrosion of BSt500$_s$ steel has direct effect on the mass loss and LCF:

1. Steel corroded for 10-90 days created a mass loss from 1.35-10.40%. For LCF loading a small mass loss created great reduction in the strength and life expectancy of steel.

2. The rib bases appeared to be inflicted first and as the corrosion level increased their size was reduced. At 90 days or 10.40% mass

loss, their average size was reduced by approximately 80% which has a direct impact on the steel-concrete bonding mechanism.
3. The fatigue limit and energy density of the corroded steel were reduced considerably due to loss of the exterior hard martensite layer. This developed stress concentration points which are highly localized at the imperfections and especially in the pits and notches of the rib bases and shortened the useful life of steel.
4. In engineering practice the gradual energy density reduction due to corrosion is overlooked by the codes and should be re-evaluated accordingly.
5. Considerable decrease of the LCF resistance of the corroded steel has a synergistic effect on the accumulated damage due to fatigue and corrosive environment.
6. The maximum load bearing capacity was reduced during LCF loading and further reduction was observed for corroded specimens. Older structures in earthquake prone areas are not expected to display a constant load bearing ability beyond a certain service life. Progression of corrosion caused significant reduction of ductility and life expectancy.

5. References

1. .Hausmann, D.A Electrochemical Behaviour of Steel in Concrete, Journal, American Concrete Institute, **1964**, 61, No. 2, 171-188.
2 .Glass, GK, Buenfeld NR., Chloride-induced corrosion of steel in concrete. *Prog. Struct. Eng. Mater,*. 2 (No. 4) , **2000**, 448-458
3. Capozucca, R. Damage to reinforced concrete due to reinforcement corrosion, *Construction and Building Materials*, Vol 9 (No. 5), **1995**, 295-303.
4. Sheng, G.M. SH.Gong, Investigation of low cycle fatigue behaviour of building structural steels under earthquake loading, *Acta Metallurgica Sinica* (English letters), 10 (1),**1997**, 51-55.
5. Tegoshi Yoshaki , *Proceedings of Academical Lectures of JAS.* Tokyo, **1983**, 606.
6. Hakuto Shigeru, Research report , Retrofitting of reinforced concrete moment Resisting Frames, supervised by Park, R and Tanaka, H. ISSN0110-3326, August **1995**.
7. Maslehuddin, M, Ibrahim IM, Huseyin S., Abdulaziz l. Al-Mana., Influence of atmospheric corrosion on the mechanical properties of reinforcing steel, *Constr Build Mater* 8 (1), **1993**, 35-41.
8. Koch, G.C. M.P. Brongers, M.P. Thompson, Y.P.Virmani, J.H. Payer, Corrosion costs and preventive strategies in the United States, Federal Highway Administration, Washington, D.C,report No.FHWA-RD, **2002**, 01-156 .
9. John P. Broomfield, *Corrosion of Steel in Concrete: Understanding, Investigationand Repair*, St. Edmundsbury Press Limited, Bury St. Edmunds, Suffolk, Great Britain, **1997**.
10. Fang, C. K. Lundgren, L. Chen, C. Zhu, Corrosion influence on bond in reinforced concrete, *Cement and Concrete Research,* Vol 34, **2004**, 2159-2167.
11. Al-Sulaimani, G.J. M. Kaleemullah, I. A.Basunbul, Rasheeduzzafar, Influence of corrosion and cracking on bond behaviour and strength of reinforced concrete members, Proc. A.C.I. 2, **1990**, 220-231 .
12. Fu, X. D.D.L. Chung, Effect of corrosion on the bond between concrete and steel rebar, *Cement and Concrete Research,* Vol 27 (No.12),**1997**, 1811-1815 .
13. Bazant, Z. P. Physical model for steel corrosion in concrete sea structures-theory, *J. Struct. Div.*, June **1979**, 1137-1153.
14. Ch. Alk. Apostolopoulos, M.P. Papadopoulos, Sp.G. Pantelakis, Tensile behaviour of corroded reinforcing steel bars BSt 500_s , *Construction and Building Material,* **2005**, In press.
15. Cairns, J. Giovanni A. Plizzari, et al., Mechanical properties of corrosion-Damaged Reinforcement, *ACI materials Journal Technical paper***,** 102-M29, V.102, No4, July-August **2005**.
16. Alvarez MG, Galvele JR., The mechanisms of pitting of high purity iron in Nacl solutions, *Corros Sci* , Vol 24, **1984**, 27-48.
17. Cabrera JG. Deterioration of concrete due to reinforcement steel corrosion, *Cement and Concrete Composite*,18 (l), **1996**, 47-59.
18. Papadakis VG., Supplementary cementing materials in concrete Activity, Durability and Planning. Danish Technological Institute concrete center, January **1999.**
19. Clementa, G. G. Testing of selected metallic reinforcing bars for extending the service life of future concrete bridges, Final report, Virginia Transp. Research Council, Charlottesville, VA, VTRC 03-R7,**2002**.
20. Ma, S.Y.M. V.V. Bertero, E.P. Popov, Experimental and Analytical Studies on the Hysteretic Behaviour of Reinforced Concrete Rectangular and T-Beams. Earthquake Eng. research report 76 (No.2),**1976**, Berkeley: Univ. of California.
21. Chai, Y.H. Incorporating low cycle fatigue model into duration-dependent inelastic design spectra, *Earthquake Engng Struct. Dyn.,* **2005**, 34, 83-96 .
22. Krawinkler, H. Performance assessment of steel components, *Earthquake Spectra* **1987**, 3 (1), 27-41.
23. Fuchs H.O and Stephens R.I. Metal fatigue in engineering. USA: John Wiley & sons Inc, **1980,** 76-82.
24. Krawinkler, H. A. Nassar, Seismic Design based on ductility and cumulative damage demands and capacities, Nonlinear seismic analysis and design of reinforced concrete buildings,Elsevier Applied Science, **1992**, 95-104.
25. Riva, P. A. Franchi and D. Tabeni ,Weld tempcore reinforcement behavior for seismic applications,materials and structures, Mater struct, Vol 34, **2001**, 240-247.
26. Franchi, A. P. Riva , P. Ronca , R. Roberti , M. La Vecchia , Failure Modalities of Reinforcement Bars in reinforced Concrete Elements Under Cyclic Loading. Studi e rocerche , Vol 17, **1996**, 157-187.
27. Almusallam, A. A. A. S. Al-Gahtani, A. R. Aziz, F. H. Dakhil, Rasheeduzzafar, Effects of reinforcement corrosion on flexural behaviour of concrete slabs, *J. of mat. in civil engineering*, 8(3), August **1996**, 123-127.
28. I. Kasiraj, I. JTP. Yao, Fatigue damage in seismic structures, *Journal of the Struct. Division (ASCE)* **1969**, 95(8), 1673-1692.
29. Morinaga, S. Prediction of Service Lives of Reinf. Concrete Build. based on Corros. Rate of Reinforcing Steel, Proc. 5th Intern. Conf. on Durability of Build. Materials and Components, Brighton, U. K., Nov. **1990**; Edited by J.M. Baker, P.J. Nixon, A.J.Majumdar, and H. Davies, 5-16, E. & F.N. SPON, London **1991**.
30. Gaidis, J.M. A.M. Rosenberg, Avoiding Corrosion Damage in Reinforced Concrete, *Concrete International,* **2001,** 23(11), 80.
31. Sih, G. C. C. K.Chao, Failure initiation in unnotched specimens subjected to monotonic and loading, *Theor. Appl. Fract. Mech.*, Vol 2,**1984**, 67-73.